Geopersia 2022, 12(1): 1-21
DOI: 10.22059/GEOPE.2021.318831.648603

RESEARCH PAPER

Geochemical Characterization of the Oil Source Rocks in the Ahwaz Oilfield, Southwestern Iran

Mona Safi, Masood Alipour-Asll*

Faculty of Earth Sciences, Shahrood University of Technology, Shahrood, Iran

Received: 10 February 2021, Revised: 13 June 2021, Accepted: 26 June 2021

Abstract
The Ahwaz oilfield is located in the Dezful embayment of the Zagros fold-thrust belt in SW Iran. The oil source rocks predominantly with the argillaceous lithologies include the Kazhdumi, Gurpi, and Pabdeh formations as well as the basal part of the Asmari Formation. The concentrations of the major, trace, and rare earth elements (REEs) of these lithologies were determined using x-ray fluorescence spectroscopy (XRF) and inductively coupled plasma-emission/mass spectrometer (ICP-ES/MS), in order to infer the geochemical characteristics of the oil source rocks. The North American Shale Composite (NASC)-normalized major oxides displayed a positive anomaly in CaO, negative anomalies in other oxides and no anomaly in P2O5. According to the spider diagram of normalized trace element, there was enrichment in V, Ni, Cu, Cd, Pb, and Th values. In the NASC-normalized REEs pattern, the oil source rocks mostly display a smooth distribution shape, negative cerium anomaly, and slightly positive anomaly in the middle rare earth elements (MREEs: Sm-Ho) values. The concentration of V, Ni, Co, and their ratios suggested a mixed marine and terrigenous source input. The ratios of redox-sensitive elements such as Ni/Co, V/Ni, V/V+Ni, Th/U, and Ce/Ce* suggested that the oil source rocks were mainly deposited under anoxic condition.

Keywords: Geochemistry, Oil source rocks, Ahwaz oilfield, Zagros, Iran.

Introduction

The oil source rocks are organic matter-rich sedimentary rocks with oil generating potential (Tissot and Welte, 1984). Type of organic materials, depositional environment, climate change, and redox condition have been shown to play effective roles in the concentration of trace elements (e.g., V, Ni, and Co) and REEs in the oil source rocks (Lewan, 1984; Barwise, 1990; Udo et al., 1992; Akinlua et al., 2010; Wang et al., 2015). Accordingly, REEs, which are relatively immobile, generally exhibit similar chemical properties from the provenance to the depositional setting (Henderson, 1984). The oil source rocks have been extensively studied by rock eval pyrolysis and biomarkers while the geochemical characteristics of the rock matrix (especially REEs) have been rarely investigated.

The most important feature of the Zagros zone is the occurrence of the supergiant oilfields, which makes it one of the most prolific region worldwide (Alavi, 2004, 2007). Dezful Embayment as a part of the Zagros zone has 45 oilfields, some of which e.g., Ahwaz, Mansuri, Agha-Jari, Rag-e-Safid, and Marun are categorized as supergiant oilfield (Fig. 1). Several oil source rock formations with various geological ages are deposited in the Ahwaz and other oilfields in the southwestern Iran, including the Gadvan (Barremian-Aptian), Kazhdumi

* Corresponding author e-mail: masoodalipour@shahroodut.ac.ir

(Aptian-Albian), Gurpi (Campanian-Masstrichtian), Pabdeh (Paleocene-Oligocene), and the basal shale of the Asmari (Oligocene-Miocene) formations (Fig. 2; McCord, 1974; Bordenave and Burwood, 1990; Bordenave and Hegre, 2010). Several studies have been conducted on the source rock formations in the Ahwaz as well as in the other oilfields of the Zagros fold-thrust zone (e.g., Bordenave and Sahabi, 1971; Bordenave et al., 1970; Bordenave and Nili, 1973; Bordenave and Hegre, 2010). The petroleum systems of the Zagros fold belt and offshore Iran were investigated using pyrolysate data, $\delta^{13}C$ and $\delta^{34}S$ isotopes of various source rocks and crude oil samples (e.g., Bordenave and Hegre, 2010; Rabbani and Bagheri-Tirtashi, 2010). According to the obtained results, the Kazhdumi and Pabdeh formations were found as the main effective source rocks, which reached the onset of oil expulsion 1 to 10 Myr after the beginning of the Zagros folding, while the Gadvan and Gurpi formations were found as the subordinate source rocks in this region (Bordenave and Burwood, 1990, 1995; Bordenave, 2002; Bordenave and Hegre, 2010; Rabbani and Bagheri-Tirtashi, 2010). The potential of source rocks of the Darquain field in the Abadan plain of the Zagros Basin was evaluated based on the rock eval pyrolysis and biomarker data. The results indicated that the early Cretaceous sequences (Garau, Gadvan, and Kazhdumi formations) have the potential of oil source. These sources predominantly contain a mixture of marine with less amount of terrigenous organic matter. Biomarker characteristics also suggested that the organic matter was deposited in a marine environment under reducing conditions (Zeinalzadeh et al., 2017).

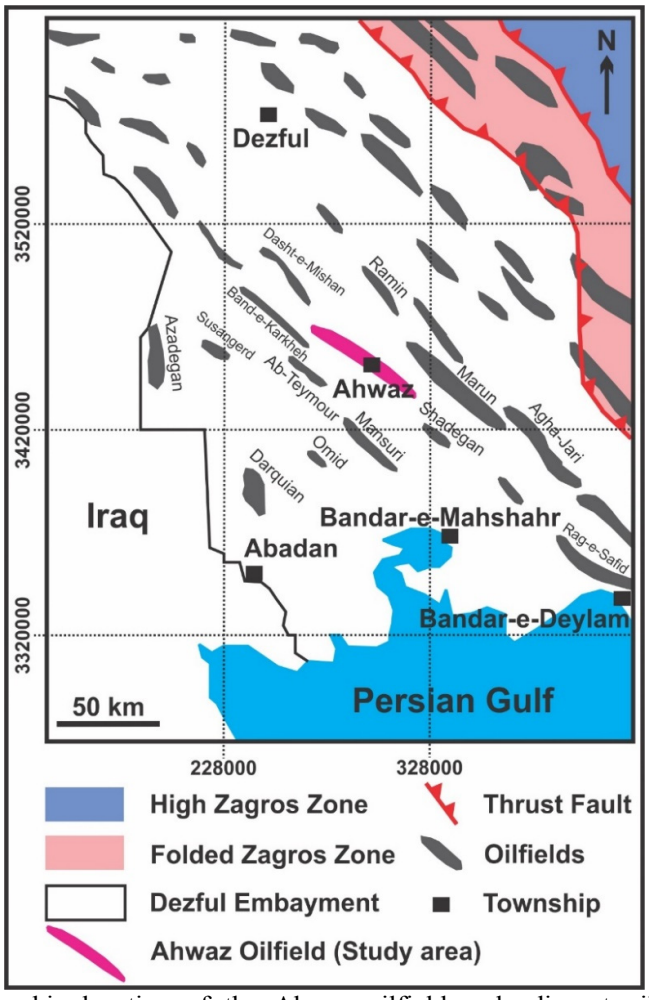

Figure 1. The geographic location of the Ahwaz oilfield and adjacent oilfields in the Dezful Embayment, Southwest of Iran

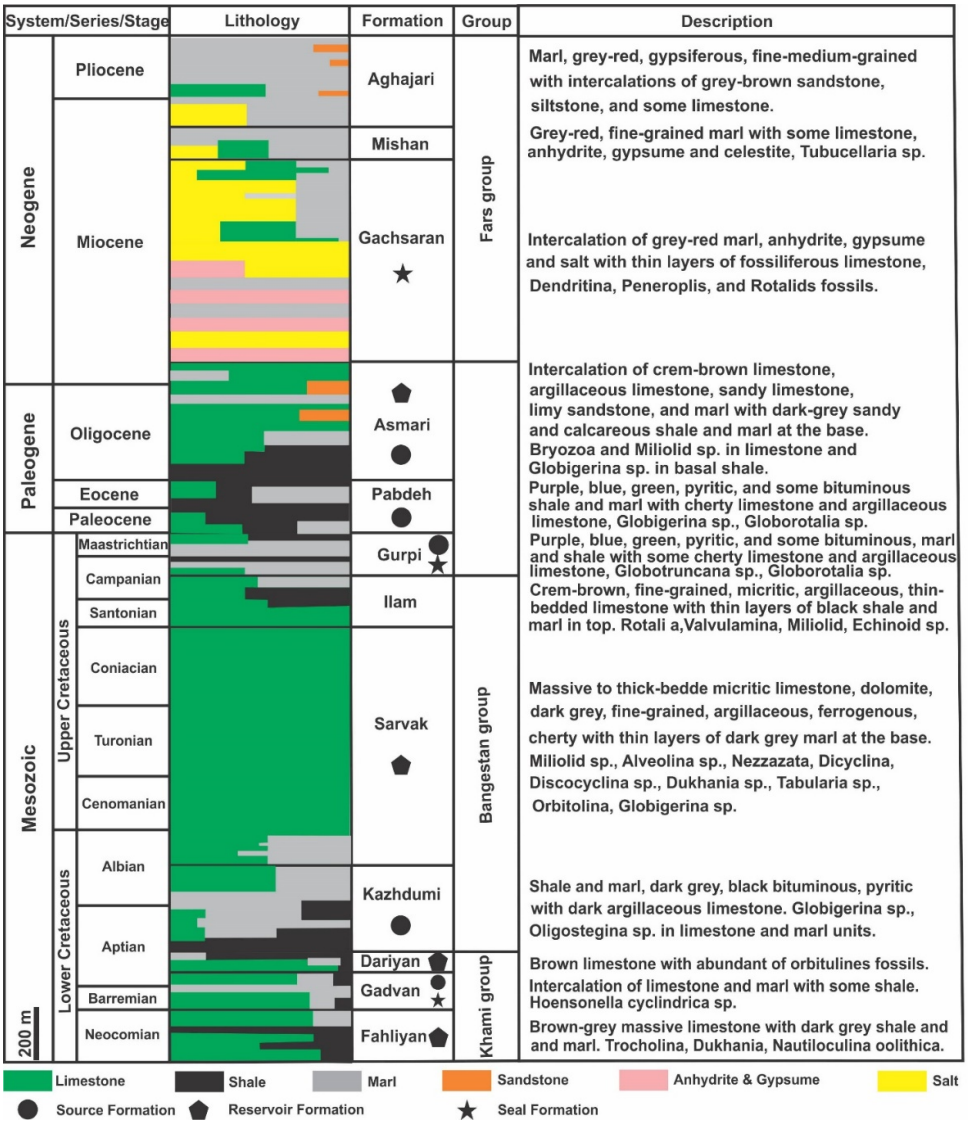

Figure 2. Schematic stratigraphy and source, reservoir, seal relationships for the Ahwaz oilfield (Safi, 2019)

The geological and geochemical studies on the rock samples from drilling cores have shown that the basal shale of the Asmari Formation in the Ahwaz oilfield has also oil generation potential (Heidari-Fard et al., 2017). Furthermore, the geochemical investigation of both V and Ni elements has already been done on crude oil samples of the Bibi-Hakimeh, Mansuri, Ab-Teymour, and Ahwaz oilfields. V and Ni concentrations and their ratios in rocks have been used to determine the paleoenvironmental conditions (Heidari-Fard, 2002, Valinejad-Khiaban, 2015; Mehrabi-Rashnou, 2017). Despite studies performed on source rock formations in the Zagros fold-thrust belt, including geological, rock eval pyrolysis, and biomarker, there is no data on the geochemical evaluations of trace and rare earth elements of the oil source rocks in the Ahwaz and other oilfields of Zagros.

In this research, we presented the major, trace, and rare earth elements data of the Kazhdumi, Gurpi, Pabdeh, and Asmari formations from five boreholes in the Ahwaz oilfield. This research aimed to apply the trace and rare earth elements geochemistry for the assessment of provenance, tectonic setting, depositional environment, and paleo-redox conditions of the oil source rocks in the Ahwaz Field.

Geological setting

The study area is located in the Zagros Basin, south and southwestern Iran. The NW-SE trending Zagros fold-thrust belt distance is extended from the NE Turkey through South Iran (Falcon, 1974; Haynes & McQuillan, 1974). Moreover, the thickness of the stratigraphic rock units in Zagros reaches more than 10 km (Alavi, 2004; Sherkati & Letouzey, 2004). The Zagros Orogeny occurred as a result of the Neotethys closure during the collision of the Arabian Plate and Iran microcontinents from the latest Cenomanian to late Eocene-Oligocene (Takin, 1972; Berberian and King, 1981; Agard et al., 2005; Ballato et al., 2010; Agard et al., 2011; Navidtalab et al., 2016; Navidtalab et al., 2020). The Zagros fold–thrust belt is subdivided into five tectono-stratigraphic domains including Fars, Dezful EmbaymentIzeh, Abadan plain and Lurestan (Stöcklin, 1968; Falcon, 1974; Berberian and King, 1981; Motiei, 1993). The Ahwaz oilfield is situated in the Dezful Embayment (Fig. 1). The main source rocks such as the Kazhdumi, Gurpi, Pabdeh, and the basal shales of the Asmari formations, playing an important role in the charge of oil reserves in the Ahwaz and other oilfields of the Dezful embayment (Bordenave and Burwood, 1990; Bordenave and Huc, 1995; Heidari-Fard et al., 2017). The Kazhdumi Formation consists of dark grey, black bituminous calcareous shale, and marl with dark argillaceous limestone. In addition, the Gurpi Formation lies over an erosional disconformity on the top of the Ilam Formation, which gradually changes to the purple shales of the overlying Pabdeh Formation. The Gurpi Formation consists of purple, blue, green, and bituminous marl and shale with some cherty limestones and argillaceous limestones. The Paleocene-Oligocene Pabdeh Formation composed of dark-gray, green, and blue marl and shale with argillaceous limestone (James and Wynd, 1965). Notably, the Asmari Formation with Oligocene-Miocene age consists of cream-brown limestone, argillaceous limestone, sandy limestone, limy sandstone with dark grey calcareous shale and marl at the base. The basal part of the Asmari Formation in the Ahwaz Field is mainly composed of dark grey calcareous shale and marl (McCord, 1974). Fig. 2 shows a schematic stratigraphy, geological descriptions, and source, reservoir, and seal relationships along with log characteristics of the Ahwaz oilfield.

Materials and methods

A total of 13 rock samples were collected from the oil source rocks in five wells of the Ahwaz oilfield named AZ-67, AZ-101, AZ-220, AZ-234, and AZ-296. The details of all these samples are presented in Table 1. All samples were collected and then stored in plastic bags. Thereafter, the samples were crushed for geochemical analyses and then powdered to less than 200 mesh.

Table 1. Concentrations of major oxides (wt.%) in 13 samples from the oil source rocks in the Ahwaz oilfield by X-Ray Fluorescence (XRF) method

Field No.	Serial No.	Well	Depth (m)	Formation	SiO_2	Al_2O_3	Fe_2O_3	MgO	CaO	Na_2O	K_2O	TiO_2	P_2O_5	MnO	SO_3	L.O.I.
AZ-67-4304	AZ-01	AZ-67	4304	Kazhdumi	6.39	1.66	0.81	0.62	43.74	0.85	0.54	0.22	0.16	0.03	2.24	39.40
AZ-101-4360	AZ-02	AZ-101	4360	Kazhdumi	17.56	5.41	1.27	0.68	35.47	0.36	1.28	0.27	0.15	0.02	2.91	31.23
AZ-101-4420	AZ-03	AZ-101	4420	Kazhdumi	42.17	18.25	6.77	1.07	6.29	0.47	0.91	0.30	0.09	0.05	2.42	17.77
AZ-220-3010	AZ-04	AZ-220	3010	Pabdeh	22.34	3.77	1.64	2.29	34.76	0.68	1.25	0.16	0.17	0.03	1.05	31.37
AZ-220-3118	AZ-05	AZ-220	3118	Pabdeh	11.19	2.42	1.50	0.80	43.07	0.79	1.31	0.12	0.12	0.03	0.84	36.64
AZ-220-3228	AZ-06	AZ-220	3228	Gurpi	10.14	2.98	1.36	0.55	44.15	0.59	1.00	0.12	0.12	0.02	0.81	37.25
AZ-234-2960	AZ-07	AZ-234	2960	base of Asmari	51.37	15.80	6.39	2.64	4.81	1.16	3.16	1.00	0.11	0.05	1.19	11.76
AZ-234-3110	AZ-08	AZ-234	3110	Pabdeh	24.89	5.24	2.30	1.18	29.25	1.30	1.43	0.25	2.27	0.02	3.10	27.64
AZ-234-3160	AZ-09	AZ-234	3160	Pabdeh	16.62	3.94	1.76	1.33	38.14	0.96	1.18	0.19	0.13	0.02	1.20	33.42
AZ-296-2868	AZ-10	AZ-296	2868	base of Asmari	34.88	11.29	5.83	4.91	16.71	0.36	2.88	0.60	0.13	0.05	1.84	20.34
AZ-296-2976	AZ-11	AZ-296	2976	Pabdeh	39.04	1.86	1.21	0.81	27.65	0.30	0.53	0.09	0.85	0.02	1.44	25.98
AZ-296-3032	AZ-12	AZ-296	3032	Pabdeh	23.17	2.19	1.50	0.97	37.00	0.56	0.85	0.10	0.14	0.02	0.46	32.26
AZ-296-3058	AZ-13	AZ-296	3058	Gurpi	11.88	2.21	1.28	0.94	42.54	0.77	1.58	0.13	0.14	0.02	0.60	36.16
NASC (Gromet et al., 1984)					64.80	16.90	5.65	2.86	3.63	1.14	3.97	0.70	0.13	0.06	0.14	
UCC (Taylor and McLennan, 1985)					65.89	15.17	4.49	2.20	4.19	3.89	3.39	0.50	0.20	0.07	0.16	

The x-ray fluorescence spectroscopy (XRF) was used to determine the whole rock major oxides, including SiO_2, Al_2O_3, Fe_2O_3, MgO, CaO, Na_2O, K_2O, TiO_2, P_2O_5, MnO, SO_3, and L.O.I. The detection limit of XRF method (XF700 equipment and fusion procedure) for all major oxides, SO_3 and L.O.I., was as 0.01, 0.002, and 0.1%, respectively. Furthermore, the major, trace, and rare earth elements, including Si, Al, Fe, Mg, Ca, Na, K, Ti, P, S, Ag, As, Ba, Be, Bi, Cd, Co, Cr, Cs, Cu, Ga, Hf, In, Li, Mn, Mo, Nb, Ni, Pb, Rb, Re, Sb, Sc, Se, Sn, Sr, Ta, Te, Th, Tl, U, V, W, Y, Zn, Zr, and REEs were determined by Ultra Trace ICP-ES/MS (MA250). A 0.25 g split is heated in HNO_3, $HClO_4$, and HF for fuming and drying. The residue was dissolved in HCl and then all the elements were analyzed by this instrument. The detection limit of ICP-ES/MS for all elements are presented in Tables 3 and 4. Both of the XRF and ICP-ES/MS analyses were performed at the ACME Labs in Canada. The precision of these analytical techniques was calculated by Thompson and Howarth method (1978) using the results of duplicate samples. As well, all elements showed the error values ≤10% at the 95% confidence level.

Results

Major elements geochemistry

The whole rock major oxides, i.e., SiO_2, Al_2O_3, Fe_2O_3, MgO, CaO, Na_2O, K_2O, TiO_2, P_2O_5, MnO, SO_3, and L.O.I. were measured for 13 samples from the source rocks in the Ahwaz oilfield (Table 1). Among the major oxides, Na_2O, CaO, MgO, K_2O, and to some extent SiO_2, Fe_2O_3, MnO, and P_2O_5 are mobile, while Al_2O_3 and TiO_2 are immobile. The CaO, SiO_2, and Al_2O_3 are the most abundant major oxides in the rock samples of the Ahwaz oilfield, respectively. The CaO content ranges from 4.81% (AZ-07; base of the Asmari Formation) to 44.15% (AZ-08; calcareous shale of the Gurpi Formation). The SiO_2 content varies from 6.39% (AZ-01; limestone of the Kazhdumi Formation) to 51.37% (AZ-07; calcareous shale and marl of the base of the Asmari Formation). The L.O.I. varies from 11.76% (AZ-07; base of the Asmari) to 39.40% (AZ-01; the Kazhdumi Formation). It is important to mention that the L.O.I. in the studied samples is affected by both calcareous and organic matters. The Al_2O_3 content varies from 1.66% (AZ-01) to 18.25% (AZ-03) in calcareous shale and marl of the Kazhdumi Formation. The Fe_2O_3 content varies from 0.81% (AZ-01) to 6.77% (AZ-03) of the Kazhdumi Formation, and MgO content ranges from 0.55% (AZ-06; marly shale of the Gurpi Formation) to 4.91% (AZ-10; sandy limestone of the Asmari Formation). The K_2O content varies from 0.53% (AZ-11; siliceous calcareous shale of the Pabdeh Formation) to 3.16% (AZ-07; base of the Asmari Formation), and Na_2O content ranges from 0.30% (AZ-11) to 1.30% (AZ-08) in calcareous shale of the Pabdeh Formation. The amount of SO_3 also increases from limestone to calcareous shale. P_2O_5 (0.09 to 2.27%), TiO_2 (0.09 to 1.00%), and MnO (0.02 to 0.05%) have very low concentrations in the samples, and their values is high in calcareous shale and limestone (Table 1).

In order to study the geochemical characteristics of the source rocks from the Ahwaz oilfield, the concentrations of major oxides in the selected samples from the Kazhdumi, Gurpi, Pabdeh, and basal shale of the Asmari formations were normalized to those of from the North American Shale Composite (NASC: Gromet et al., 1984). The results show that the amount of CaO in all samples is higher than NASC, P_2O_5 value is close to NASC, and the contents of other oxides are lower than NASC (Figs. 3a-d). In addition, the distribution pattern of elements in shale of the Kazhdumi Formation is similar to basal shale of the Asmari Formation (Figs. 3a, d).

The Si value and Al/Si ratio reflect high quartz, clay, and feldspar content (Potter, 1978; Li et al., 2018). The Al/Si ratio in the oil source rocks of the Ahwaz Field ranges from 0.06 in calcareous shale to 0.46 in argillaceous limestone and calcareous shale (Table 2).

The Ca/Si ratio in the source rocks varies from 0.17 in shale to 11 in limestone and argillaceous limestone, indicating high possible calcareous content compared to quartz and clay minerals in these rocks (Table 2). In the Al_2O_3-SiO_2-CaO ternary diagram (He et al., 2016), most of the studied samples from the Ahwaz Field are located in the carbonate-rich corner (Fig. 4a). In the Log (TFe_2O_3/K_2O) vs. Log (SiO_2/Al_2O_3) diagrams (Herron, 1988), the selected samples fall in the shale area, and few samples show wacke and litharenite due to the high siliceous content (Fig. 4b). There is no typical shale in the study area and based on < 10% Al_2O_3, the selected samples are marl to argillaceous limestone.

Table 2. Concentrations of major (wt.%) and trace (ppm) elements in 13 samples from the oil source rocks in the Ahwaz oilfield by ICP-ES/MS method

Field No.	Serial No.	Si	Al	Fe	Mg	Ca	Na	K	Ti	P	S	Ag	As	Ba	Be	Bi
Detection limit		0.01	0.01	0.01	0.01	0.01	0.00	0.01	0.00	0.00	0.04	0.02	0.20	1.00	1.00	0.04
AZ-67-4304	AZ-01	2.99	1.05	0.80	0.59	32.41	0.81	0.26	0.04	0.06	0.81	0.26	5.30	73.00	0.75	0.05
AZ-101-4360	AZ-02	8.21	2.26	1.34	0.53	25.23	0.21	0.75	0.06	0.05	0.97	6.15	23.80	68.00	2.00	0.13
AZ-101-4420	AZ-03	19.71	9.00	4.95	0.65	4.30	0.33	0.70	0.60	0.05	1.48	12.38	34.30	80.00	2.00	0.31
AZ-220-3010	AZ-04	10.44	2.35	1.31	1.30	25.26	0.46	0.68	0.11	0.07	0.71	0.28	3.70	283.00	0.75	0.10
AZ-220-3118	AZ-05	5.23	1.55	1.16	0.49	31.96	0.72	0.70	0.10	0.04	0.48	0.17	2.50	332.00	0.75	0.08
AZ-220-3228	AZ-06	4.74	1.90	1.05	0.34	32.25	0.51	0.54	0.09	0.04	0.51	0.18	4.70	257.00	0.75	0.07
AZ-234-2960	AZ-07	24.01	9.09	5.59	1.74	4.11	0.91	2.98	0.61	0.06	0.93	0.13	12.90	461.00	2.00	0.25
AZ-234-3110	AZ-08	11.64	2.73	1.98	0.71	22.43	0.83	0.92	0.17	1.07	1.45	0.62	5.60	118.00	0.75	0.19
AZ-234-3160	AZ-09	7.77	2.96	1.65	0.92	33.09	0.84	0.79	0.16	0.06	0.79	0.31	4.90	744.00	0.75	0.11
AZ-296-2868	AZ-10	16.31	5.44	4.29	2.90	10.38	0.20	1.98	0.32	0.06	1.21	0.10	3.90	212.00	2.00	0.18
AZ-296-2976	AZ-11	18.25	1.06	0.85	0.48	20.76	0.19	0.33	0.06	0.37	0.75	0.44	2.60	312.00	0.75	0.19
AZ-296-3032	AZ-12	10.83	1.53	1.47	0.58	32.66	0.47	0.61	0.08	0.06	0.39	0.42	1.90	1030.00	0.75	0.32
AZ-296-3058	AZ-13	5.55	1.30	0.94	0.51	29.44	0.74	0.76	0.10	0.05	0.31	0.21	1.60	151.00	0.75	0.07
*UCC		30.75	8.03	3.14	1.32	2.99	2.89	2.81	0.30	0.09	0.06	0.05	1.50	550.00	3.00	0.16

Field No.	Serial No.	Cd	Co	Cr	Cs	Cu	Ga	Hf	In	Li	Mn	Mo	Nb	Ni	Pb	Rb
Detection limit		0.02	0.20	1.00	0.10	0.10	0.02	0.02	0.01	0.10	1.00	0.05	0.04	0.10	0.02	0.10
AZ-67-4304	AZ-01	1.28	2.20	84.00	0.80	27.20	2.19	0.32	0.01	7.80	231.00	16.97	1.22	49.20	100.20	11.90
AZ-101-4360	AZ-02	0.90	3.60	85.00	1.90	267.50	6.81	0.20	0.03	22.10	127.00	8.50	6.10	37.20	5671.38	39.80
AZ-101-4420	AZ-03	0.60	17.50	121.00	1.80	278.50	22.13	2.70	0.08	166.60	377.00	8.02	21.13	55.40	4562.70	77.60
AZ-220-3010	AZ-04	0.27	6.70	60.00	1.80	23.50	5.42	0.90	0.04	15.00	225.00	2.39	3.91	50.90	53.92	24.90
AZ-220-3118	AZ-05	0.16	6.10	51.00	1.20	41.20	3.72	0.60	0.01	11.60	174.00	1.80	3.15	49.20	28.24	20.30
AZ-220-3228	AZ-06	0.20	3.70	43.00	1.20	35.50	4.22	0.65	0.03	11.80	104.00	4.93	2.77	18.70	43.60	17.90
AZ-234-2960	AZ-07	0.28	24.00	116.00	4.10	31.20	24.83	4.87	0.09	64.80	505.00	3.56	19.60	61.30	99.20	78.20
AZ-234-3110	AZ-08	9.15	8.60	126.00	2.30	62.00	6.99	1.38	0.04	21.10	129.00	22.64	6.73	92.50	34.51	35.10
AZ-234-3160	AZ-09	0.52	8.40	75.00	1.90	27.30	7.12	1.77	0.05	19.70	155.00	4.96	6.09	64.30	38.44	31.30
AZ-296-2868	AZ-10	0.19	14.70	62.00	2.30	84.30	13.70	2.81	0.06	37.40	354.00	1.77	11.03	32.70	74.91	51.90
AZ-296-2976	AZ-11	0.55	3.90	53.00	0.80	205.60	2.67	0.25	0.03	12.00	58.00	2.89	2.12	41.10	72.23	11.00
AZ-296-3032	AZ-12	0.38	8.00	31.00	0.90	234.60	3.81	0.53	0.03	15.40	139.00	1.73	2.62	25.60	82.44	15.30
AZ-296-3058	AZ-13	0.25	5.80	42.00	1.00	61.90	3.13	0.63	0.02	10.20	145.00	0.62	3.43	41.90	81.97	17.70
*UCC		0.10	17.00	85.00	4.60	25.00	17.00	5.80	0.05	20.00	500.00	1.50	12.00	44.00	17.00	112.00

Field No.	Serial No.	Re	Sb	Sc	Se	Sn	Sr	Ta	Te	Th	Tl	U	V	W	Y	Zn
Detection limit		0.00	0.02	0.10	0.30	0.10	1.00	0.10	0.05	0.10	0.05	0.10	2.00	0.10	0.10	0.20
AZ-67-4304	AZ-01	0.08	2.09	2.00	5.30	0.40	1602.00	0.08	8.31	1.00	0.58	10.60	131.00	0.60	8.20	197.00
AZ-101-4360	AZ-02	0.07	8.63	3.30	5.30	3.60	1255.00	0.50	0.90	0.80	1.30	7.40	69.00	5.00	6.90	162.60
AZ-101-4420	AZ-03	0.00	5.12	12.10	1.10	3.30	492.00	1.40	0.30	8.70	2.09	2.30	125.00	1.90	13.90	207.90
AZ-220-3010	AZ-04	0.02	1.31	5.60	1.30	0.60	974.00	0.20	6.00	2.40	0.26	2.20	72.00	0.60	10.60	44.20
AZ-220-3118	AZ-05	0.01	1.27	4.30	0.60	0.50	1002.00	0.20	8.84	1.70	0.18	1.40	38.00	0.50	9.50	20.70
AZ-220-3228	AZ-06	0.01	0.95	3.40	1.10	0.70	886.00	0.20	8.02	2.10	0.22	2.40	39.00	0.60	10.00	35.80
AZ-234-2960	AZ-07	0.00	2.32	17.10	0.70	3.00	255.00	1.40	0.64	12.30	0.56	3.10	131.00	2.70	29.80	129.10
AZ-234-3110	AZ-08	0.13	3.57	6.00	9.00	0.90	1122.00	0.30	5.41	3.40	1.45	10.50	306.00	0.60	12.80	153.00
AZ-234-3160	AZ-09	0.03	1.02	6.00	2.80	0.90	1285.00	0.40	8.12	3.60	0.31	5.00	67.00	0.50	13.70	155.90
AZ-296-2868	AZ-10	0.00	1.13	9.60	0.80	1.60	383.00	0.80	3.56	8.80	0.42	2.30	73.00	1.50	20.80	45.10
AZ-296-2976	AZ-11	0.02	1.94	2.40	3.10	0.40	760.00	0.08	4.94	1.00	0.19	2.10	56.00	1.00	4.70	75.40
AZ-296-3032	AZ-12	0.00	1.58	3.80	1.00	0.70	629.00	0.20	6.88	1.70	0.11	1.60	45.00	0.60	10.80	48.60
AZ-296-3058	AZ-13	0.01	1.13	3.80	0.70	0.50	786.00	0.20	6.72	1.50	0.13	1.40	30.00	0.50	9.20	24.50
*UCC		0.00	0.20	13.60	0.05	5.50	350.00	1.00	0.00	10.70	0.75	2.80	107.00	2.00	22.00	71.00

Table 2. Continuation of Table 2

Field No.	Serial No.	Zr	Al/Si	Ca/Si
Detection limit		0.20		
AZ-67-4304	AZ-01	10.80	0.35	10.85
AZ-101-4360	AZ-02	8.00	0.28	3.07
AZ-101-4420	AZ-03	95.30	0.46	0.22
AZ-220-3010	AZ-04	30.70	0.23	2.42
AZ-220-3118	AZ-05	23.30	0.30	6.11
AZ-220-3228	AZ-06	21.70	0.40	6.80
AZ-234-2960	AZ-07	162.50	0.38	0.17
AZ-234-3110	AZ-08	52.70	0.23	1.93
AZ-234-3160	AZ-09	60.10	0.38	4.26
AZ-296-2868	AZ-10	100.70	0.33	0.64
AZ-296-2976	AZ-11	2.30	0.06	1.14
AZ-296-3032	AZ-12	18.70	0.14	3.02
AZ-296-3058	AZ-13	23.70	0.23	5.30
*UCC		190.00		

*Upper Continental Crust (UCC) from Taylor and McLennan, 1985.

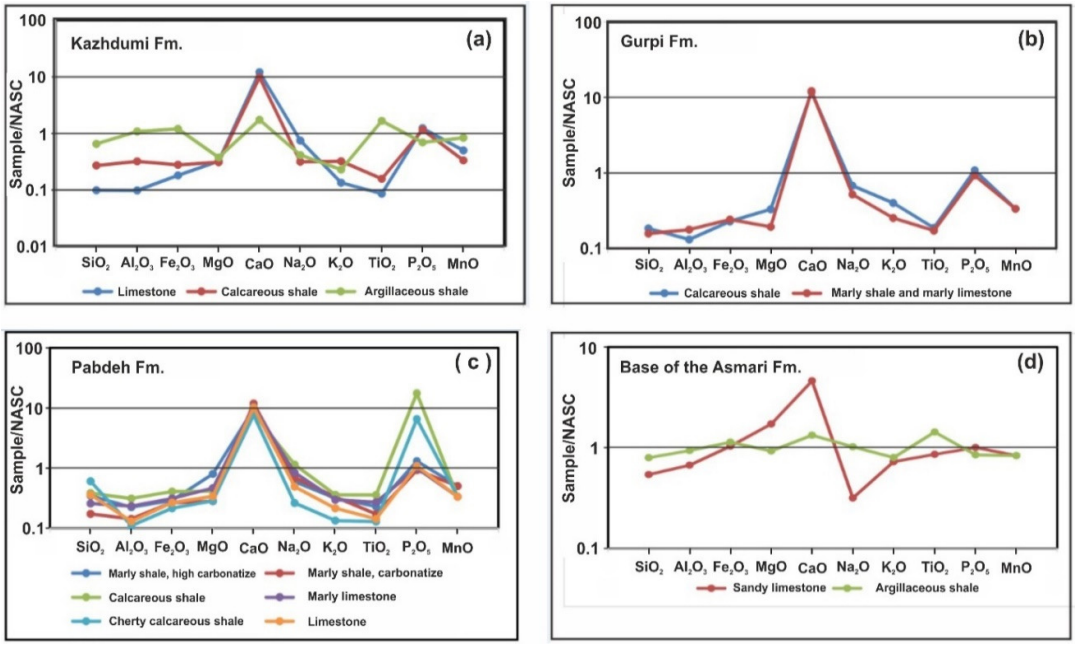

Figure 3. NASC-normalized major oxides patterns of the oil source rocks in the Ahwaz Field. (a) Pabdeh Formation, (b) base of the Asmari Formation, (c) Kazhdumi Formation, and (d) Gurpi Formation

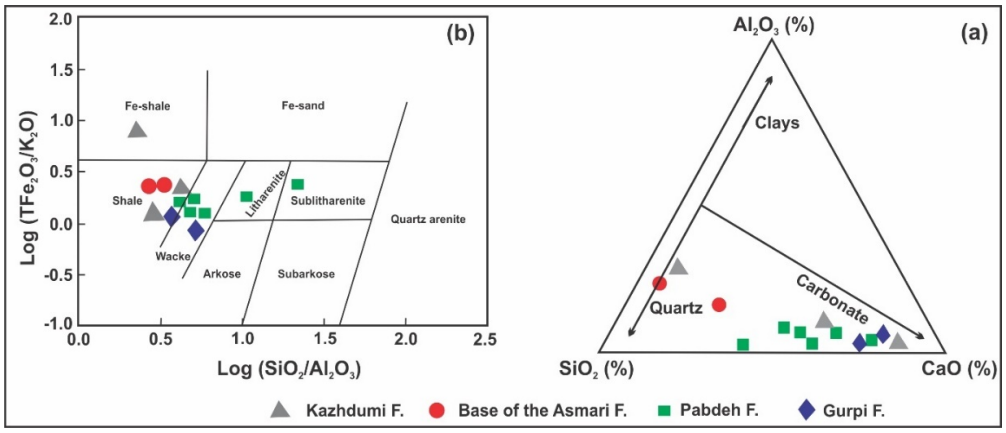

Figure 4. (a) Ternary diagram showing relative proportions of major elements in oil source formations at the Ahwaz field (He et al. 2016), (b) lithology classification of rock samples from the study area (Herron 1988)

Trace elements geochemistry

The concentration of trace elements in the studied samples from the oil source rocks of the Ahwaz Field are presented in Table 2. The concentration of trace elements was normalized to the upper continental crust (UCC; Taylor and McLennan, 1985; Fig5). The Th value of the shale and marl of the Kazhdumi Formation (in well AZ-03) is quite similar to the basal shale of the Asmari Formation (Figs. 5a, b).

The Ni, V, and Co as biophile elements may be applied as a correlation factor in the study of oil source rocks and paleoenvironmental conditions (Barwise, 1990; Udo et al., 1992; Akinlua et al., 2007). The concentration of Ni ranges from 37.20 to 55.40 ppm (average 47 ppm), 18.70 to 41.90 ppm (average 30 ppm), 25.60 to 92.50 ppm (average 54 ppm), and 32.70 to 61.30 ppm (average 47 ppm) in the Kazhdumi, Gurpi, Papdeh formations and the base of the Asmari Formation, respectively.

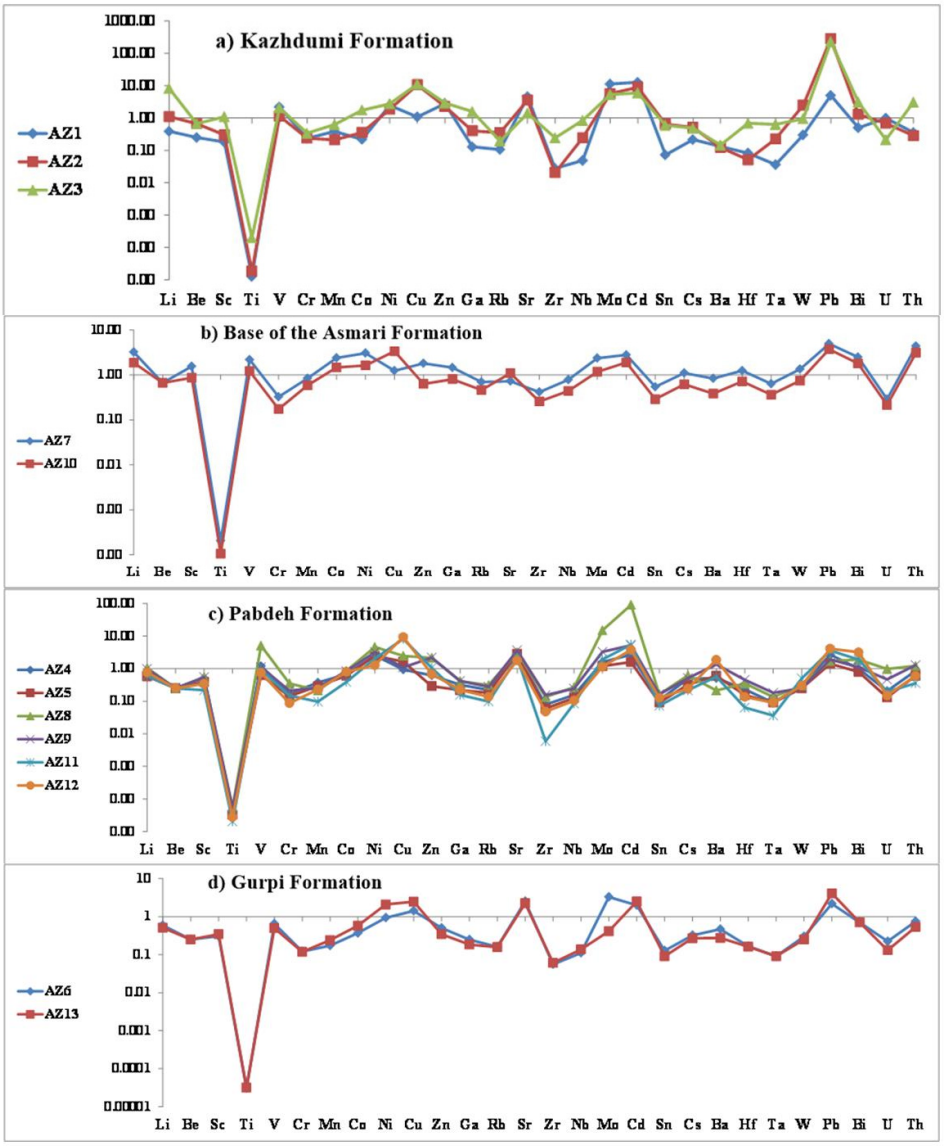

Figure 5. The upper continental crust (UCC)-normalized minor and trace elements patterns of the oil source rocks in the Ahwaz Field. (a) Pabdeh Formation, (b) base of the Asmari Formation, (c) Kazhdumi Formation, and (d) Gurpi Formation

The Co concentration ranges from 2.20 to 17.50 (8) ppm for Kazhdumi, 3.70 to 5.80 (5) ppm for Gurpi, 3.90 to 8.60 (7) ppm for Pabdeh, and 14.70 to 24.00 (19) ppm for the base of the Asmari Formation. The concentration of V ranges from 69 to 131 (108) ppm for Kazhdumi, 30 to 39 (35) ppm for Gurpi, 38 to 306 (97) ppm for Pabdeh, and 73 to 131 (102) ppm for the base of the Asmari Formation (Table 2). The distribution of the trace elements (Fig. 6) shows that vanadium is the most abundant trace element in the source rocks, and its content in the Kazhdumi and the base of the Asmari is higher than the Pabdeh and Gurpi formations. Nickel has the same averages in the Kazhdumi, Pabdeh formations, and the base of the Asmari Formation, and its value is reduced in the Gurpi Formation. Cobalt had the lowest concentration in all formations, and its value is reduced from the base of the Asmari, Kazhdumi, and Pabdeh formation to the Gurpi Formation, respectively.

Rare earth elements geochemistry (REEs)

The concentration of rare earth elements (REEs) in samples of the Ahwaz oilfield is presented in Table 3. The content of ∑REE in samples varies from 22.09 ppm in calcareous shale (AZ-11 sample) of the Pabdeh Formation to 226.81 ppm in shale (AZ-07 sample) from the base of the Asmari Formation with an average of 72.03 ppm, and all samples (exclude AZ-07) have lower ∑REE concentration than the North American Shale Composite (NASC: 173.21 ppm, Gromet et al. 1984). This indicates that oil source rock formations in the study area are depleted in REEs.

Table 3. Concentrations of rare earth elements (ppm) in 13 samples from the oil source rocks in the Ahwaz oilfield by ICP-MS method

Serial No.	AZ-01	AZ-02	AZ-03	AZ-04	AZ-05	AZ-06	AZ-07	AZ-08	AZ-09	AZ-10	AZ-11	AZ-12	AZ-13	NASC*
Formation	Kazhdumi	Kazhdumi	Kazhdumi	Pabdeh	Pabdeh	Gurpi	base of Asmari	Pabdeh	Pabdeh	base of Asmari	Pabdeh	Pabdeh	Gurpi	
La	4.70	4.90	23.90	10.40	8.90	10.40	43.60	13.40	15.20	29.80	5.20	11.00	8.70	32.00
Ce	7.04	8.89	61.52	15.83	13.34	14.15	94.71	25.39	25.90	60.55	8.23	15.17	13.25	73.00
Pr	1.50	1.30	7.60	2.40	1.90	2.50	11.00	3.30	3.60	7.70	1.20	2.20	1.90	7.90
Nd	5.20	5.50	29.40	9.50	7.00	8.00	43.50	13.30	13.30	29.40	3.90	8.60	7.70	33.00
Sm	1.10	1.20	6.50	1.70	1.50	1.50	9.20	2.80	2.90	6.20	0.80	1.80	1.60	5.70
Eu	0.30	0.30	1.20	0.40	0.30	0.30	1.80	0.60	0.50	1.20	0.20	0.40	0.30	1.24
Gd	1.00	1.50	4.50	1.20	1.20	1.30	7.30	2.20	1.80	4.30	0.60	1.40	1.30	5.20
Tb	0.20	0.10	0.80	0.30	0.30	0.30	1.10	0.40	0.40	0.70	0.10	0.30	0.20	0.85
Dy	1.00	0.90	3.80	1.40	1.10	1.30	6.00	2.30	2.10	4.20	0.70	1.70	1.30	5.80
Ho	0.20	0.20	0.70	0.30	0.30	0.30	1.10	0.40	0.40	0.80	0.10	0.30	0.30	1.04
Er	0.70	0.70	1.90	0.90	0.80	0.70	3.40	1.30	1.30	2.30	0.40	0.90	0.80	3.40
Tm	0.08	0.08	0.30	0.10	0.10	0.10	0.50	0.20	0.20	0.30	0.08	0.10	0.08	0.50
Yb	0.60	0.50	1.60	0.90	0.80	0.80	3.20	1.10	1.20	2.10	0.50	1.00	0.70	3.10
Lu	0.08	0.08	0.20	0.10	0.08	0.08	0.40	0.20	0.20	0.30	0.08	0.10	0.08	0.48
∑REE	23.70	26.15	143.92	45.43	37.62	41.73	226.81	66.89	69.00	149.85	22.09	44.97	38.21	173.21
LREE	18.44	20.59	122.42	38.13	31.14	35.05	192.81	55.39	58.00	127.45	18.53	36.97	31.55	
MREE	3.80	4.20	17.50	5.30	4.70	5.00	26.50	8.70	8.10	17.40	2.50	5.90	5.00	
HREE	1.46	1.36	4.00	2.00	1.78	1.68	7.50	2.80	2.90	5.00	1.06	2.10	1.66	
LREE/HREE	12.63	15.14	30.61	19.07	17.49	20.86	25.71	19.78	20.00	25.49	17.48	17.60	19.01	
Ce/Ce*	0.57	0.77	0.99	0.69	0.70	0.60	0.94	0.83	0.76	0.87	0.72	0.67	0.71	
Eu/Eu*	1.26	0.97	0.96	1.22	0.98	0.94	0.96	1.06	0.94	1.01	1.26	1.10	0.91	
Pr/Pr*	1.49	1.14	1.11	1.20	1.22	1.45	1.06	1.11	1.20	1.13	1.32	1.19	1.16	

*NASC from Gromet et al., 1984

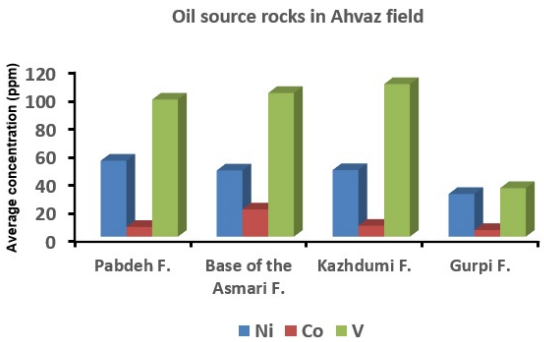

Figure 6. Distribution of nickel, cobalt, and vanadium in the oil source rocks (Pabdeh, base of the Asmari, Kazhdumi, and Gurpi Formations) from Ahwaz field

The comparison of REE contents in the studied formations shows that average concentration of each REEs in the base of the Asmari Formation is relatively higher than the Kazhdumi, Pabdeh, and Gurpi formations, and the REE values reduced from the base of the Asmari toward the Kazhdumi, Pabdeh, and Gurpi formations, respectively (Figs. 7a-c). The average content of LREE (La-Nd) in the Kazhdumi, Gurpi, Pabdeh formations, and the base of the Asmari Formation is 53.82, 33.30, 39.69, and 160.13 ppm, respectively. The average content of middle REEs (Sm-Ho) in the Kazhdumi, Gurpi, Pabdeh, formations, and the base of the Asmari Formation is 8.50, 5.00, 5.87, and 21.95 ppm, respectively. The average content of heavy REEs (Er-Lu) in the Kazhdumi, Gurpi, Pabdeh, formations, and the base of the Asmari Formation is 2.27, 1.67, 2.11, and 6.25 ppm, respectively (Table 3 and Fig. 7d).

The distribution pattern of NASC-normalized REE for the four formations is shown in figure 8. The smooth pattern of REE indicates poor separation between light and heavy rare earth elements, so the LREE/HREE ratio in the selected samples varies from 12.63 to 30.61 (average 20.07). In addition, concentrations of REEs in most of samples are lower than NASC. Only the REE concentrations in the shale and marls of the Kazhdumi (AZ-03) and the base of the Asmari Formation (AZ-07) show slight enrichment relative to the NASC. In the Ahwaz Field, all samples from the oil source formations show negative Ce_N anomalies, and all samples with Eu/Eu* ≈ 1 have neither positive nor negative Eu_N anomalies (Table 3, Figs. 8a-d).

Relation of REEs with trace elements

The correlation coefficients between ΣREE and trace elements concentrations are shown in Table 4. Bivariate statistical analysis based on geochemical data in a logarithmic scale indicates that there is significant positive correlation ($r > 0.70$, at the 99% confidence level) between Be, Co, Cs, Ga, Hf, Li, Nb, Rb, Sc, Ta, Th, Y, and Zr with ΣREE, very poor positive correlation between Ba, Pb, and Zn with ΣREE, and a negative correlation between Sr, U, and Cu with ΣREE for the Kazhdumi, Gurpi, Pabdeh formations, and the base of the Asmari Formation of the Ahwaz Field (Table 4).

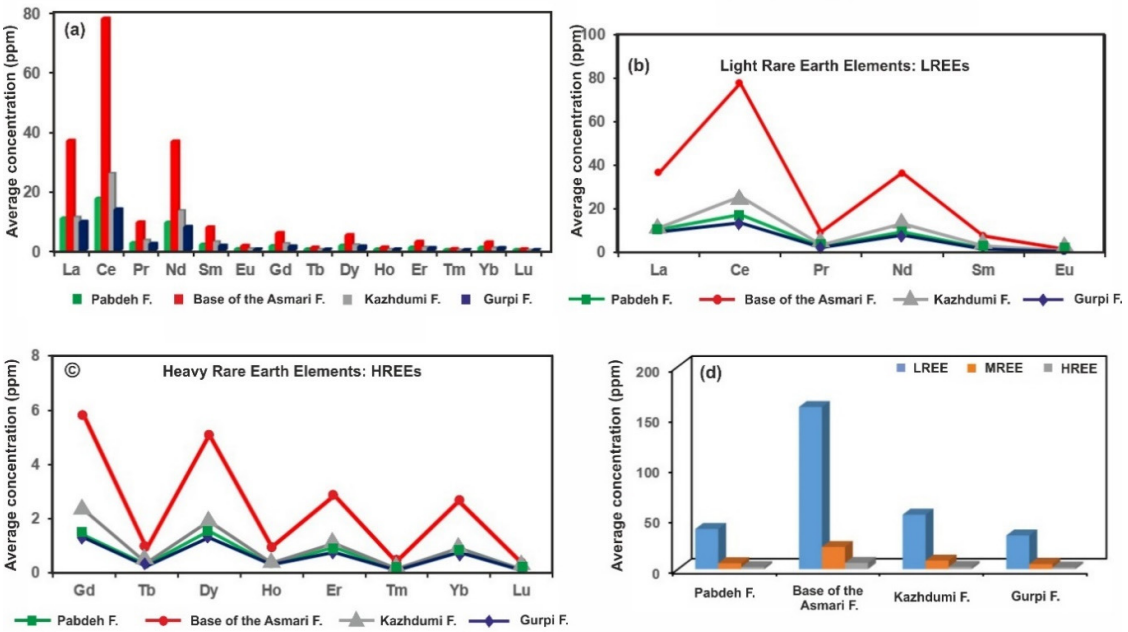

Figure 7. The average concentration of REE (ppm) in the oil source formations from the Ahwaz field: (a) REEs (La-Lu), (b) LREEs (La-Eu), (c) HREEs (Gd-Lu), and (d) LREE (La-Nd), MREE (Sm-Ho), and HREE (Er-Lu)

Table 4. Pearson's correlation coefficient matrix between trace and rare earth elements based on log geochemical data of oil source rocks (n = 13) in the Ahwaz oilfield

Element	Ba	Be	Co	Cr	Cs	Cu	Ga	Hf	Li	Nb	Ni	Pb	Rb	Sc	Sr	Ta	Th	U	V	Y	Zn	Zr	∑REE
Ba	1.00																						
Be	-0.32	1																					
Co	0.29	0.57	1																				
Cr	-0.50	0.52	0.37	1																			
Cs	0.01	0.65	**0.74**	0.66	1																		
Cu	-0.20	0.39	0.07	-0.06	-0.18	1																	
Ga	-0.05	**0.82**	**0.87**	0.63	**0.85**	0.14	1																
Hf	0.22	0.45	**0.91**	0.46	**0.76**	-0.26	0.83	1															
Li	-0.13	**0.80**	**0.82**	0.61	0.68	0.34	**0.96**	**0.73**	1														
Nb	-0.07	**0.80**	**0.88**	0.62	**0.86**	0.17	**0.98**	**0.81**	**0.93**	1													
Ni	-0.19	0.03	0.33	**0.75**	0.44	-0.24	0.30	0.37	0.28	0.36	1												
Pb	-0.58	**0.70**	0.08	0.39	0.15	0.67	0.43	-0.09	0.57	0.42	-0.03	1											
Rb	0.04	0.68	0.68	0.53	**0.96**	-0.15	**0.77**	0.68	0.57	**0.80**	0.32	0.13	1										
Sc	0.14	0.65	**0.96**	0.51	**0.85**	-0.06	**0.94**	**0.94**	**0.86**	**0.94**	0.37	0.15	**0.78**	1									
Sr	-0.27	-0.62	**-0.81**	-0.09	-0.49	-0.20	**-0.69**	**-0.68**	**-0.67**	**-0.67**	0.10	-0.09	-0.49	**-0.75**	1								
Ta	-0.05	**0.84**	**0.84**	0.55	**0.84**	0.17	**0.97**	**0.78**	**0.91**	**0.97**	0.22	0.47	**0.81**	**0.91**	**-0.66**	1							
Th	0.17	0.56	**0.93**	0.47	**0.77**	-0.14	**0.89**	**0.98**	**0.81**	**0.85**	0.29	0.01	0.68	**0.96**	**-0.75**	**0.82**	1						
U	-0.48	0.07	-0.27	0.66	0.23	-0.15	0.01	-0.10	-0.04	-0.01	0.45	0.17	0.20	-0.14	0.48	-0.02	-0.12	1					
V	-0.39	0.28	0.30	**0.87**	0.52	-0.06	0.45	0.39	0.44	0.41	**0.71**	0.16	0.39	0.38	-0.04	0.33	0.41	**0.73**	1				
Y	0.24	0.50	**0.85**	0.39	**0.79**	-0.31	**0.78**	**0.93**	0.63	**0.75**	0.25	-0.10	**0.78**	**0.89**	-0.68	**0.78**	**0.92**	-0.02	0.36	1			
Zn	-0.37	0.38	0.10	**0.80**	0.33	0.17	0.39	0.15	0.45	0.34	0.50	0.50	0.22	0.18	0.10	0.32	0.18	**0.78**	**0.77**	0.12	1		
Zr	0.13	0.45	**0.85**	0.44	**0.77**	-0.31	**0.80**	**0.95**	0.67	**0.79**	0.34	-0.04	**0.71**	**0.90**	-0.55	**0.80**	**0.92**	-0.03	0.37	**0.95**	0.12	1	
∑REE	0.16	**0.73**	**0.95**	0.47	**0.80**	-0.08	**0.91**	**0.97**	**0.83**	**0.89**	0.43	0.08	**0.74**	**0.97**	**-0.78**	**0.88**	**0.99**	-0.11	0.39	**0.94**	0.20	**0.92**	1

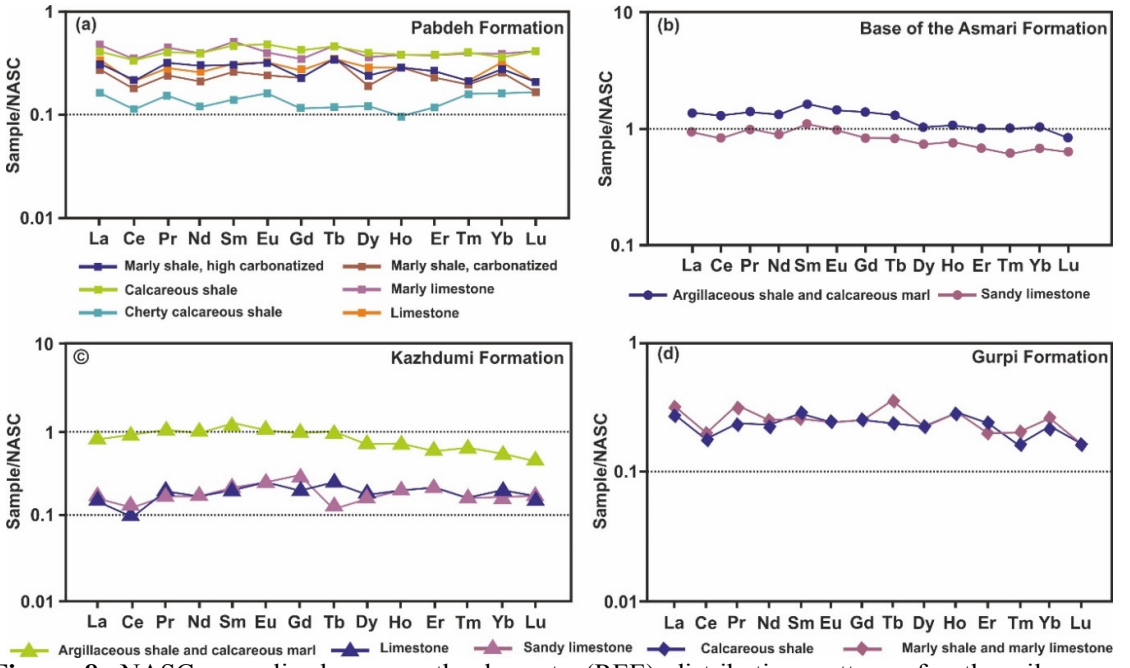

Figure 8. NASC-normalized rare earth elements (REE) distribution patterns for the oil source formations of Ahwaz field. Normalization values are taken from Gromet et al. (1984)

Discussion

Provenance

The major and trace elements geochemistry provides valuable information about the provenance of sedimentary rocks. For example, the Al_2O_3/TiO_2 ratio for sediments derived from the mafic, intermediate, and felsic igneous rocks ranges from 3 to 8, 8 to 21, and 15 to 70, respectively (Girty et al., 1996; Hayashi et al., 1997; Cullers, 2002). In the Ahwaz oil source

rocks, the Al_2O_3/TiO_2 ratio ranges from 16 to 49 (average 32), indicates a felsic to intermediate parent rock (Table 5). In the TiO_2 vs. Al_2O_3 and TiO_2 vs. Zr scatter plots (Hayashi et al., 1997), samples are located in felsic to intermediate igneous rocks (Figs. 9a, b). Trace element ratios, such as Th/Cr, La/Th, Th/Sc, and Zr/Sc vary in felsic, mafic, and ultramafic source rocks (Floyd and Leveridge, 1987; McLennan et al., 1993; Armstrong-Altrin et al., 2012). Th/Cr ratio in sediments derived from the felsic and mafic source rocks ranges from 0.13 to 2.7 and 0.018 to 0.046, respectively (Armstrong-Altrin et al., 2016). Th/Cr ratio in the oil source rock samples from the Ahwaz oilfield ranges from 0.01 to 0.14, indicating that they may have probably been derived from the intermediate igneous rocks (Table 5). A scatter plot of La/Th vs. Hf (Floyd and Leveridge, 1987) suggests an andesitic to felsic parent rocks with some basic rocks (Fig. 9c). The cross plot of Zr/Sc vs. Th/Sc (McLennan et al., 1993) suggests that the studied samples were derived from felsic to intermediate igneous rocks (Fig. 9d).

Table 5. Selected ratios of major and trace elements of oil source rocks from the Ahwaz Field for provenance and and palaeoenvironment study

Serial No.	Formation	Al_2O_3/TiO_2	K_2O/Na_2O	Cr/Ni	Ni/Co	Th/Co	Th/Cr	Th/U	V/Cr	V/Ni	V/(V+Ni)	V/(Ni+Ni)
AZ-01	Kazhdumi	27.67	0.62	1.71	22.36	0.45	0.01	0.09	1.56	2.66	0.73	1.33
AZ-02	Kazhdumi	49.18	3.56	2.28	10.33	0.22	0.01	0.11	0.81	1.85	0.65	0.93
AZ-03	Kazhdumi	15.73	1.94	2.18	3.17	0.50	0.07	3.78	1.03	2.26	0.69	1.13
AZ-04	Pabdeh	23.56	1.84	1.18	7.60	0.36	0.04	1.09	1.20	1.41	0.59	0.71
AZ-05	Pabdeh	20.17	1.66	1.04	8.07	0.28	0.03	1.21	0.75	0.77	0.44	0.39
AZ-06	Gurpi	24.83	1.69	2.30	5.05	0.57	0.05	0.88	0.91	2.09	0.68	1.04
AZ-07	base of Asmari	15.80	2.72	1.89	2.55	0.51	0.11	3.97	1.13	2.14	0.68	1.07
AZ-08	Pabdeh	20.96	1.10	1.36	10.76	0.40	0.03	0.32	2.43	3.31	0.77	1.65
AZ-09	Pabdeh	20.74	1.23	1.17	7.65	0.43	0.05	0.72	0.89	1.04	0.51	0.52
AZ-10	base of Asmari	18.82	8.00	1.90	2.22	0.60	0.14	3.83	1.18	2.23	0.69	1.12
AZ-11	Pabdeh	20.67	1.77	1.29	10.54	0.26	0.02	0.48	1.06	1.36	0.58	0.68
AZ-12	Pabdeh	21.90	1.52	1.21	3.20	0.21	0.05	1.06	1.45	1.76	0.64	0.88
AZ-13	Gurpi	17.00	2.05	1.00	7.22	0.26	0.04	1.07	0.71	0.72	0.42	0.36

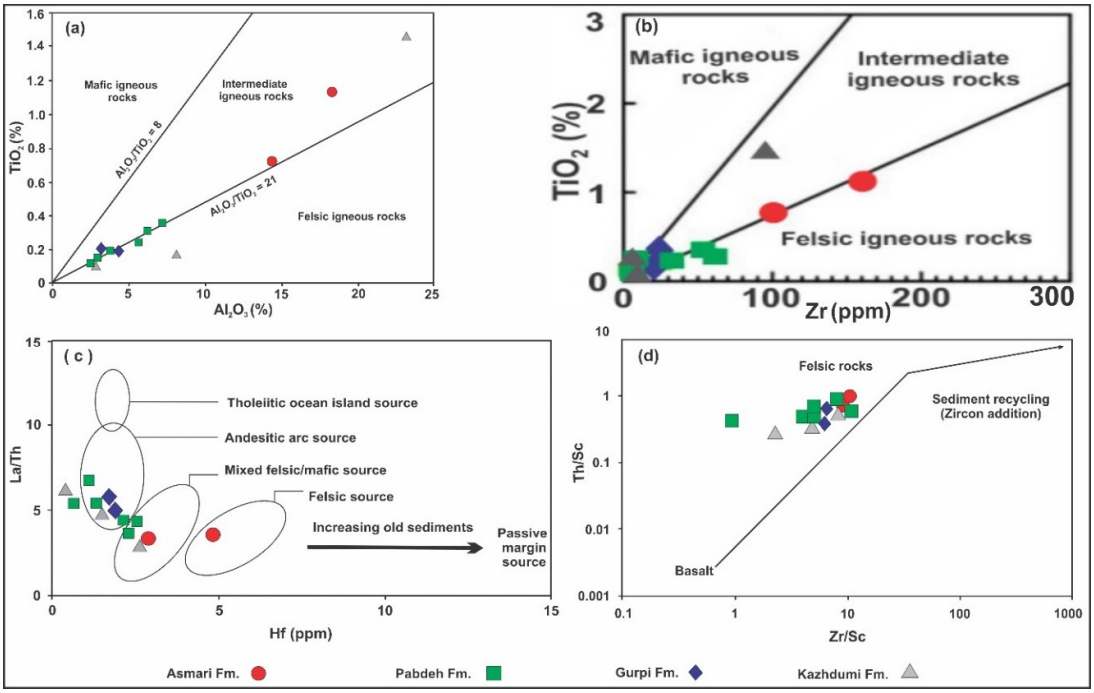

Figure 9. (a) TiO_2 vs. Al_2O_3 diagram (Hayashi et al., 1997), (b) TiO_2 vs. Zr diagram (Hayashi et al. 1997) to determine the geochemical composition of provenance igneous rocks in Ahwaz oilfield, (c) La/Th vs. Hf bivariate plot (Floyd and Leveridge, 1987), and (d) Th/Sc vs. Zr/Sc bivariate plot (McLennan et al., 1993) for the Ahwaz oil source formations samples

Therefore, various geochemical criteria indicate that the oil source rocks in the Ahwaz oilfield are mainly originated from felsic to intermediate igneous parent rocks.

Depositional setting

Trace elements concentration and their ratios in petroleum source rocks have been used in assessing the origin, redox condition, and depositional environment (Udo et al., 1992; Galarraga et al., 2008; Akinlua et al., 2010; Xie et al., 2018). In the V vs. Al_2O_3 cross plot (after Mortazavi et al., 2013), samples are mostly located in the shallow marine and fluvial environments and suggest that the deposition of oil source formations in the Ahwaz oilfield is performed in shallow marine environment (Fig. 10). The V/Ni ratio < 1.9, 1.9 to 3, and > 3 indicate terrestrial, mixed marine-terrestrial, and marine organic matter, respectively (Galarraga et al., 2008; Akinlua et al., 2016). The V/Ni ratio in the Kazhdumi, Gurpi, Pabdeh formations, and the base of the Asmari Formation ranging from 1.85 to 2.66 (average 2.26), 0.72 to 2.09 (average 1.4), 0.77 to 3.31 (average 1.61), and 2.14 to 2.23 (average 2.18), respectively. These results indicate that mixed marine-terrestrial source for organic matter in the Ahwaz oilfield. Bivariate statistical analysis indicates that there is significant positive correlation ($r > 0.70$) between Be, Co, Cs, Ga, Hf, Li, Nb, Rb, Sc, Ta, Th, Y, and Zr with ΣREE for the studied samples (Table 4). Most of these elements such as Be, Cs, Hf, Li, Nb, Rb, Ta, Th, and Zr are lithophile elements (Goldschmidt, 1923), suggesting that REEs of the oil source formations in the study area are mainly terrigenous.

Tectonic setting

Several researchers have envisaged that tectonic settings control or influence the chemical compositions of clastic sedimentary rocks (e.g., Bhatia, 1983; Bhatia and Crook, 1986; Malaza et al., 2013). Different tectonic setting discrimination diagrams have been used to separate between different tectonic settings, and they all provide consistent results for siliciclastic rocks that have not been strongly affected by post-depositional weathering and metamorphism (Bhatia, 1983; Bhatia and Crook, 1986; Roser and Korsch, 1986). Similarly, the bivariate and ternary plots of major and trace element geochemistry have been widely used by several researchers to determine the tectonic setting of shales (Baiyegunhi et al., 2017).

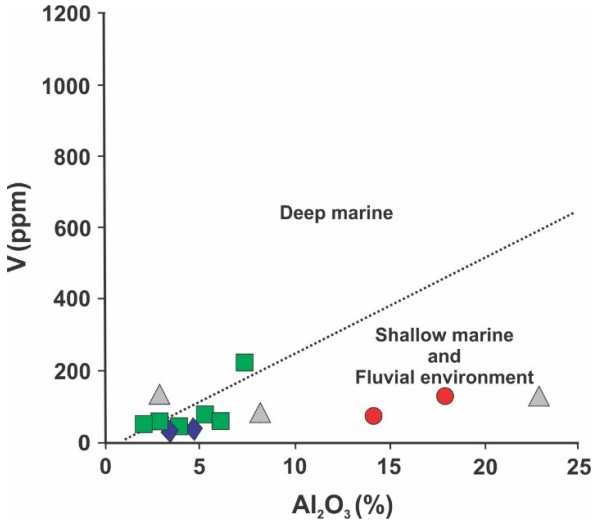

Figure 10. Scatter plot of V vs. Al_2O_3 (after Mortazavi et al. 2013), showing shallow marine and fluvial environment for deposition of the oil source formations in the Ahwaz Field

The tectonic environment of the oil source rocks in the Ahwaz oilfield investigated based on geochemical data by using various diagrams. In the Fe_2O_3+MgO vs. TiO_2 diagram (Bhatia, 1983), the Kazhdumi samples mostly plotted in the passive continental margin, samples from the Gurpi and Pabdeh formations located in the active continental margin, while samples from the Asmari Formation plotted close to the oceanic island arc area (Fig. 11a). The Log K_2O/Na_2O vs. SiO_2/Al_2O_3 diagram (Roser and Korsch, 1988) also confirms the passive continental margin for the Lower Cretaceous (Aptian-Albian) Kazhdumi Formation and active continental margin for the Upper Cretaceous (Campanian-Maastrichtian) Gurpi, and Paleocene-Oligocene Pabdeh formations in the Ahwaz Field (Fig. 11b). Two samples (AZ-11 and AZ-12) from the Pabdeh Formation due to the high content of the SiO_2/Al_2O_3 ratio are not within this diagram. Likewise, the ternary plot of Th–Sc–Zr/10 (Bhatia and Crook, 1986) indicated that the Kazhdumi Formation was deposited in a passive continental setting, while The Gurpi and Pabdeh, formations were deposited in active continental margin setting (Fig. 11c). Although samples from base of the Asmari Formation are located in the oceanic island arc (Fig. 11a) and active continental margin fields (Figs. 11b, c), but based on the available geological data the Asmari Formation was deposited in the post collision environment (e.g., Glennie, 2000; Alavi, 2007; Piryaei et al., 2010). The results of our geochemical research on the oil source rock formations are confirmed by the geological studies in the Zagros Basin and the eastern margin of the Arabian plate (e.g., Sharland et al., 2001). The Zagros Basin was a tectonically passive depositional setting from the Permian to about the latest Cenomanian (Navidtalab et al., 2016; Navidtalab et al., 2020), and it has become an active continental margin from the Upper Cretaceous to latest Eocene (Glennie, 2000). The field observations in combination with a regional set of well logs, close to the margin of the Arabian plate in the interior Fars area in Iran have recognized three tectono-sedimentary phases. These phases indicating the evolution from a passive to an active margin (Alavi, 2007; Piryaei et al., 2010; Piryaei et al., 2011; Navidtalab et al., 2020): Phase I (Late Albian–Cenomanian), during this time interval the Arabian plate still had a passive margin, and sedimentation occurred on a carbonate shelf with intra-shelf basins. Phase II (Turonian to Late Campanian, obduction phase) is characterized by major changes in depositional environments and sedimentary facies, as a result of obduction and foreland basin creation. Phase III (Late Campanian–Maastrichtian), during this phase platform carbonates developed again bordering the foreland basin in this region.

Paleoredox conditions

Based on Jones and Manning (1994), the Ni/Co ratios < 5, 5 to 7, and > 7 representing oxic, dysoxic, and suboxic to anoxic depositional conditions, respectively.

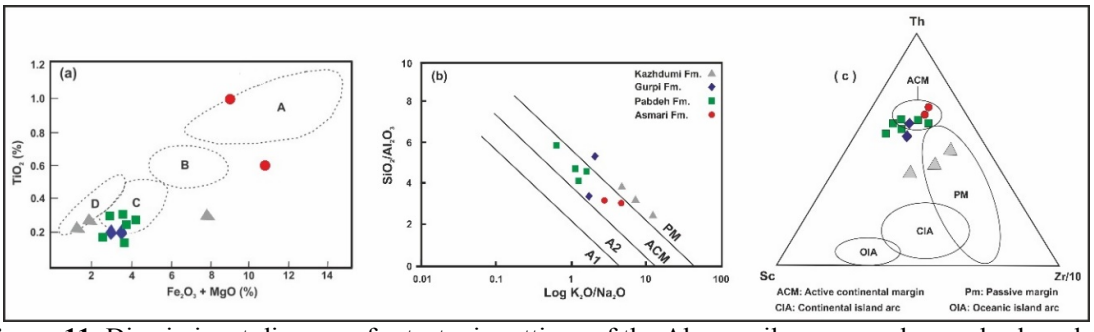

Figure 11. Discriminant diagrams for tectonic settings of the Ahwaz oil source rock samples based on major element values. (a) Fe_2O_3+MgO vs. TiO_2 (Bhatia, 1983), (b) Log K_2O/Na_2O vs. SiO_2/Al_2O_3 diagram (Roser and Korsch 1988). A and A1: Oceanic island arc; B and A2: Continental arc; C and ACM: Active continental margin; D and PM: Passive continental margin, (c) Th-Sc-Zr/10 ternary plot for the studied samples showing tectonic setting (Background field after Bhatia and Crook, 1986)

The samples from the Kazhdumi, Gurpi, Pabdeh, and base of the Asmari formations have Ni/Co ratio ranging 3.17 to 22.36 (average 11.95), 5.05 to 7.22 (average 6.14), 3.20 to 10.76 (average 7.97), and 2.22 to 2.55 (average 2.39), respectively (Table 5).

The results show that shales and marls of the Kazhdumi Formation was deposited under oxic condition, whereas the calcareous shale and argillaceous limestone part of this formation was deposited under suboxic to anoxic condition (Table 5; Fig. 12a). The sea-level variations and local differential subsidence during the Aptian-Albian controlled sediment deposition and redox conditions during sedimentation of the Kazhdumi Formation (Ghasemi-nejad et al., 2009). The UCC-normalized minor and trace elements (Fig., 5a-d) show depletion in Ti, Rb, Zr, Nb, Sn, Ta, and slightly U which is due to the fact that their contents are mainly reduced toward silt and clay fractions in the sedimentary environments, while V, Ni, Cu, Cd, and Pb increase toward silt and clay fractions (Ginsburg, 1960). The enrichment of Th in the basal shale of the Asmari Formation is possibly due to high terrigenous influx. The average Ni/Co ratio (6.14) in the studied samples indicates that the Gurpi Formation were deposited under dysoxic condition (Table 5; Fig. 12a).

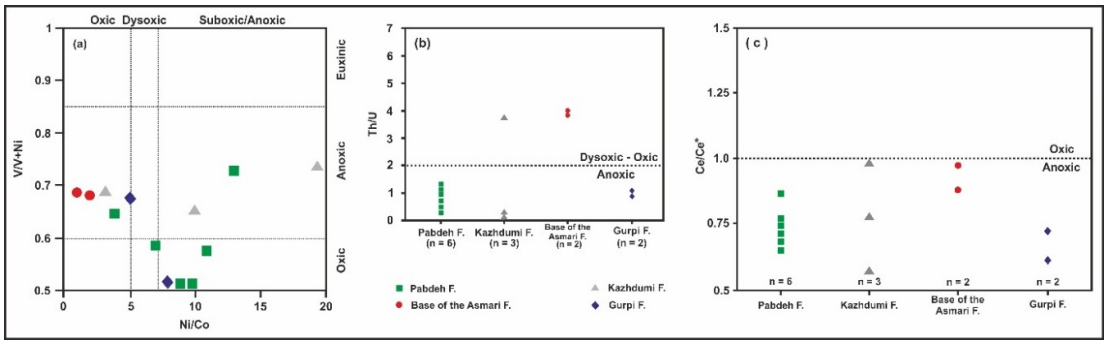

Figure 12. Distribution diagrams of redox proxies for the oil source formations: a) V/V+Ni vs. Ni/Co, b) Th/U, and c) Ce anomaly (Ce/Ce*).

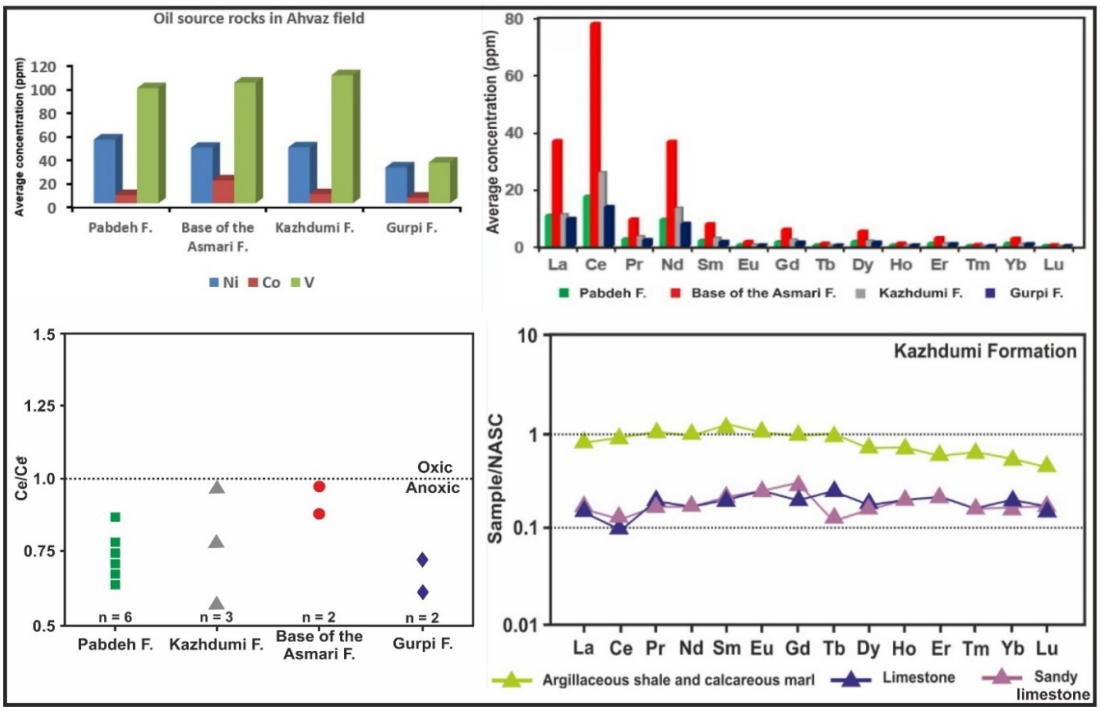

Graphical abstract

Biostratigraphy and paleoecology of the Gurpi Formation in the nearby Marun oilfield show that changing of relative abundance of morphotypes and ratio of planktonic/benthic foraminifera during the early Campanian-late Maastrichtian is related to dysoxic-anoxic conditions and low-high energy environments (Darabi and Sadeghi, 2017). The anoxic condition in the early-middle Campanian shows a transgression in basin during this time, which is correlated with a major eustatic sea level rise in the early Campanian (Haq and Shutter, 2008). Near the end of the Campanian, a decreasing in the frequency of morphotypes in the middle part of the Gurpi Formation indicates a decreasing in water depth and dysoxic condition (Darabi and Sadeghi, 2017).

The average Ni/Co ratio (7.97) of samples from the Pabdeh Formation indicates that this Formation were deposited under suboxic to anoxic conditions (Table 5; Fig. 12a). The negative carbon isotopic composition ($\delta^{13}C$: −1.85 to −4.89) of the phosphate-bearing Pabdeh Formation in the Kuhe-Lar-anticline (Zagros Basin, SW Iran) shows that it may be formed within the suboxic-to-anoxic zone (Bolourchifard et al., 2019). Based on the average Ni/Co ratio (2.39), the lower shale of the Asmari Formation was deposited under oxic conditions (Table 5; Fig. 12a). The distribution of the larger benthic foraminifera indicates that shallow marine carbonate sediments of the Oligocene-Miocene Asmari Formation in the Zagros Basin have been deposited in tropical to subtropical warm waters under oligotrophic or slightly mesotrophic conditions in a ramp environment (Sadeghi et al., 2009; Roozpeykar and Maghfouri-Moghaddam, 2016).

The ratio of V/(V+Ni) can be used as a redox condition indicator. The V/V+Ni values greater than 0.5 show anoxic environment while values less than 0.5 indicate oxic environment. The source rock samples from the Ahwaz oilfield have V/V+Ni values greater than 0.5 (Table 5, Fig. 12a), indicating that these source rocks were mainly deposited under anoxic conditions. The Th/U ratio is one of signatures that often provide information on depositional environment (Hatch and Leventhal, 1992; Rimmer, 2004). Th/U ratio of less than 2 is generally applied as a signature of anoxic condition (Wignall and Twitchett, 1996). In the source rocks of the Ahwaz Field, the Th/U ratios are in the range of 0.09 to 3.78 (average 1.33) for the Kazhdumi Formation, 0.88 to 1.07 (average 0.97) for Gurpi Formation, 0.32 to 1.21 (average 0.81) for Pabdeh Formation, and 3.83 to 3.97 (average 3.90) for the base of the Asmari Formation (Table 5). The results display that the shale sand marls of the Kazhdumi Formation and the base of the Asmari Formation were deposited under oxic conditions, whereas the calcareous shales and argillaceous limestones of the Kazhdumi, Pabdeh, and Gurpi formations were deposited under anoxic conditions (Fig. 12b). The other redox parameter such as Ce anomaly (Ce/Ce^*) suggests that all formations in the Ahwaz oilfield were deposited under anoxic condition (Fig. 12c).

Conclusions

The major, trace and rare earth elements concentrations in the Kazhdumi, Gurpi, Pabdeh formations, and the base of the Asmari Formation in the Ahwaz oilfield were measured, in order to infer the geochemical features of these oil source rocks. The distribution of elements showed that CaO is the most abundant component in the oil source rocks which followed by SiO_2 and Al_2O_3. Moreover, some major and trace element concentrations and their ratios indicated that the Aptian-Albian Kazhdumi Formation was deposited in the passive continental margin, while the Gurpi (Campanian-Masstrichtian), Pabdeh (Paleocene-Oligocene), were deposited in the active continental margin. As well, the V, Ni, and Co contents suggest a mixed marine and terrigenous source input. The enrichments of V, Ni, Cu, Cd, Pb, and Th; smooth distribution shape of REEs; negative cerium anomaly; slight enrichment of MREEs; and depletion of REEs to the NASC were found as the prominent geochemical characteristics of the studied oil source rocks. The ratios of redox-sensitive elements suggested that the basal shale of the Asmari and

some parts of the Kazhdumi formations were deposited under oxic condition. However, the Kazhdumi, Gurpi, and Pabdeh formations were deposited under anoxic conditions. Finally, besides the geology, rock eval pyrolysis, and biomarker data, the elemental characteristics of the source rocks should also be used during exploring hydrocarbon resources in the Zagros Basin and same regions worldwide.

Acknowledgements
The authors express special appreciation to the National Iranian South Oil Company (NISOC) and Shahrood University of Technology for their financial and scientific supports. We would like to appreciate Prof. Taheri, Prof. Ghasemi, and Prof. Mokhtari for their helps and comments. We are also thanks to the editorial office of Geopersia Journal and reviewers for handling and review our manuscript.

References

Agard, P., Omrani, J., Jolivet, L., Whitechurch, H., Vrielynck, B., Spakman, W., Monie, P., Meyer, B., Wortel, R., 2011. Zagros orogeny: a subduction-dominated process. Geological Magazine 148: 692-725.

Agard, P., Omrani, J., Jolivet, L., and Mouthereau, F., 2005. Convergence history across Zagros (Iran): constraints from collisional and earlier deformation. International Journal of Earth Sciences 94: 401-19.

Akinlua, A., Olise, F.S., Akomolafe, A.O., McCrindle, R.I., 2016. Rare earth element geochemistry of petroleum source rocks from northwestern Niger Delta. Marine and Petroleum Geology 77: 409-417.

Akinlua, A., Adekola, S.A., Swakamisa, O., Fadipe, O.A., Akinyemi, S.A., 2010. Trace metals characterization of Cretaceous Orange Basin hydrocarbon source rocks. Applied Geochemistry 25: 1587-1595.

Akinlua, A., Torto, N., Ajayi, T.R., 2008. Determination of rare earth elements in Niger Delta crude oils by inductively coupled plasma e mass spectrometry. Fuel 87: 1469-1477.

Akinlua, A., Torto, N., Ajayi, T.R., Oyekunle, J.A.O., 2007. Trace metals characterization of Niger Delta kerogens. Fuel 86: 1358-1364.

ALavi, M., 2007. Structures of the Zagros fold-thrust belt in Iran. American Journal of Sciences 307: 1064-1095.

Alavi, M., 2004. Regional stratigraphy of the Zagros fold-thrust belt of Iran and its proforeland evolution. American Journal of Sciences 304: 1-20.

Aouidi, S.E., Fakhi, S., Laissaoui, A., Malek, O.A., Benmansour, M., Ayach, A., Batal, Y.E., Aadjour, M., Tahri, M., Yahyaoui1, A.E., Benkdad, A., 2017. Geochemical characterization of the black shale from the Ama Fatma coastal site in the Southwest of Morocco. American Journal of Chemistry, 7(5): 153-162

Armenteros, I., Huerta, P., 2006. The role of clastic sediment influx in the Formation of Calcrete and Palustrine Facies: a response to paleographic and climatic conditions in the Southeastern Tertiary Duero Basin (Northern Spain). Geological Society of American Special Papers, 416: 119-132.

Armstrong-Altrin, J.S., Lee, Y.I., Kasper-Zubillaga, J.J., Carranza-Edwards, A., Garcia, D., Eby, N., Balaram, V., Cruz-Ortiz, N.L., 2012. Geochemistry of beach sands along the western Gulf of Mexico, Mexico: implication for provenance. Chemie der Erde-Geochemistry, 72: 345-362.

Armstrong-Altrin, J.S., Machain-Castillo, M.L., 2016. Mineralogy, geochemistry, and radiocarbon ages of deep sea sediments from the Gulf of Mexico. Journal of South American Earth Sciences, 71: 182-200.

Baiyegunhi, C., Liu, K., Gwavava, O., 2017. Geochemistry of sandstones and shales from the Ecca Group, Karoo Super group, in the Eastern Cape Province of South Africa: Implications for provenance, weathering and tectonic setting. Open Geosciences, 9: 340-360.

Ballato, P., Mulch, A., Landgraf, A., Strecker, M.R., Dalconi, M.C., Friedrich, A., Tabatabaei, S.H., 2010. Middle to late Miocene Middle Eastern climate from stable oxygen and carbon isotope data, southern Alborz mountains, N Iran. Earth and Planetary Science Letters, 300: 125-38.

Barwise, A.J.G., 1990. Role of nickel and vanadium in petroleum classification. Energy Fuel, 4: 647-

652.
Bau, M., Dulski, P., 1996. Distribution of yttrium and rare-earth elements in the Penge and Kuruman iron-formations, Transvaal Supergroup, South Africa. Precambrian Research, 79: 37-55.
Bauluz, B., Mayayo, M.J., Fernandez-Nieto, C., Manuel, J., Lopez, G., 2000. Geochemistry of Precambrian and Paleozoic siliciclastic rocks from the Iberian Range (NE Spain): implications for source-area weathering, sorting, provenance, and tectonic setting. Chemical Geology, 168: 135-150.
Berberian, M., King, G.C.P., 1981. Towards a paleogeography and tectonic evolution of Iran. Canadian Journal of Earth Sciences, 18: 1764-6.
Bhatia, M.R., 1983. Plate tectonics and geochemical composition of sandstones. Journal of Geology, 91: 611-627.
Bhatia, M.R., Crook, K.A., 1986. Trace element characteristics of graywackes and tectonic setting discrimination of sedimentary basins. Contributions to Mineralogy and Petrology, 92, 181-193.
Bolourchifard, F., Fayazi, F., Mehrabi, B., Memarkouchehbagh, A., 2019. Evidence of high-energy storm and shallow water facies in Pabdeh sedimentary phosphate deposit, Kuhe-Lar-anticline, SW Iran. Carbonate and Evaporite, 34 (4): 1703-1721.
Bordenave, M.L., Hegre, J.A., 2010. Current distribution of oil and gas fields in the Zagros fold belt of Iran and contiguous offshore as the result of petroleum systems. Geological Society Special Publication, 330: 291-353.
Bordenave, M.L., 2002. The Middle Cretaceous to Early Miocene Petroleum System in the Zagros Domain of Iran, and its prospect evaluation. Presented at the AAPG Convention, Houston, 10-13 March 2002 (extended abstract).
Bordenave, M.L., Burwood, R., 1995. The Albian Kazhdumi Formation of the Dezful Embayment, Iran. One of the most efficient petroleum generating systems in Petroleum Source Rocks Series: case books in Earth Sciences. Ed. by Katz B.J., Springer Verlag, Heiderberg, pp. 183-207.
Bordenave, M. L., Burwood, R., 1990. Source rock distribution and maturation in the Zagros orogenic belt; provenance of the Asmari and Bangestan reservoir oil accumulations. Organic Geochemistry, 16: 369-387.
Bordenave, M.L., Huc, A.Y., 1995. The Cretaceous source rocks in the Zagros foothills of Iran. Oil and Gas Science and Technology, 50(6): 727-752.
Bordenave, M. L., Nili, A.R., 1973. Geochemical project, review and appraisal of the Khuzestan Province. Geology and Exploration Division, Iranian Oil Operating Companies, Report 1194.
Bordenave, M.L., Sahabi, F., 1971. Geochemical project, appraisal of Lurestan. Geology and Exploration Division, Iranian Oil Operating Companies, Report 1182.
Bordenave, M.L., Combaz, A., Giraud, A., 1970. Influence de l'origine des matie`res organiques et de leur degre´ d'e´volution sur les produits de pyrolyse du ke´roge`ne. In: HOBSON, G. D. & SPEARS, G. C. (eds) Adv. Organic Geochemistry, 389-405.
Cullers, R.L., 2002. Implications of elemental concentrations for provenance, redox conditions, and metamorphic studies of shales and limestones near Pueblo, CO, USA. Chemical Geology, 191: 305-327.
Darabi, G., Sadeghi, A., 2017. Biostratigraphy and Paleoecology of the Gurpi Formation in Marun Oil Field, Zagros Basin, SW Iran. Geopersia, 7 (2): 169-198.
Falcon, N.L., 1974. Southern Iran: Zagros Mountains. In Mesozoic-Cenozoic orogenic belts: Data for orogenic studies (ed. A. M. Spencer), pp. 199-211. Geological Society of London, Special Publication, no. 4.
Floyd, P.A., Leveridge, B.E., 1987. Tectonic environment of the Devonian Gramscatho Basin, South Cornwall: Framework mode and geochemical evidence from turbiditic sandstones. Journal of the Geological Society of London, 144: 531-542.
Galarraga, F., Llamas, J.F., Martinez, A., Martinez, M., Marquez, G., Reategui, K., 2008. V/Ni ratio as a parameter in palaeoenvironmental characterization of nonmature medium-crude oils from several Latin American basins. Journal of Petroleum Science and Engineering, 61: 9-14.
Ghasemi-Nejad, E., Head, M.J., Naderi, M., 2009. Palynology and petroleum potential of the Kazhdumi Formation (Cretaceous: Albian-Cenomanian) in the South Pars field, northern Persian Gulf. Marine and Petroleum Geology, 26: 805-816.
Ginsburg, I., 1960. Principles of geochemical prospecting. Translated by V.P. Sokoloff, New York and London, Pergamon, 311 pp.

Girty, G.H., Ridge D.L., Knaack, C.H., Johnson, D., AL-riyami, R.K., 1996. Provenance and depositional setting of Paleozoic chert and argillite Sierra Nevada, California. Journal of Sedimentary Research, 66: 107-118.

Glennie, K.W., 2000. Cretaceous tectonic evolution of Arabia's eastern plate margin: a tale of two oceans. In: A Lsharhan, A.S. and Scott, R.W. (eds) Middle East Models of Jurassic/Cretaceous Carbonate Systems. SEPM Special Publication, 69: 9-20.

Goldschmidt, V.M., 1923. Geochemische verteilungsgesetze der elements (I). Videnskapsselskapets Skrifter. I. Mat. Naturv. Klasse. 3: 1-17.

Haq, B.U., Schutter, S.R., 2008. A chronology of Paleozoic sea-level changes: Science 322: 64-68.

Hatch, J.R., Leventhal, J.S., 1992. Relationship between inferred redox potential of the depositional environment and geochemistry of the Upper Pennsylvanian (Missourian) Stark Shale Member of the Dennis Limestone, Wabaunsee County, Kansas, USA. Chemical Geology, 99: 65-82.

Hayashi, K.I., Fujisawa, H., Holland, H.D., Ohmoto, H., 1997. Geochemistry of ~1.9 Ga sedimentary rocks from northeastern Labrador, Canada. Geochimica et Cosmochimica Acta, 61: 4115-4137.

Haynes, S.J., McQuillan, H., 1974. Evolution of the Zagros suture zone, Southern Iran. Geological Society of American Bulletin, 85: 739-44.

He, C., Ji, L., Wu, Y., Wu, Y., Ao, S., Zhang, M., 2016. Characteristics of hydrothermal sedimentation process in the Yanchang Formation, South Ordos Basin, China: Evidence from element geochemistry. Sedimentary Geology, 345: 33-41.

Heidari-Fard, M.H., 2002. Nickel and Vanadium in Oils of Asmari and Bangestan Pools in Bibi-Hakimeh Oilfield. M.Sc. thesis, Shahid Chamran University of Ahwaz, Ahwaz, Iran, 120 pp. (in Persian with English abstract)

Heidari-Fard, M.H., Saran, M., Kalani, M., Saraf-Dokht, H., 2017. Geochemical study of base shale of the Asmari Formation in Ahwaz field (A10 and A11 Zones). National *Iranian* South Oil Company (NISOC), Internal Report, 135 pp. (in Persian with English abstract)

Henderson, P., 1984. General geochemical properties and abundances of the rare earth elements. In: Denderson, P. (Ed.), Rare Earth Element Geochemistry. Elsevier, New York, pp. 1-32.

Herron, M.M., 1988. Geochemical classification of terrigenous sands and shales from core or log data. Journal of Sedimentary Research, 58: 820-829.

James, G.A., Wynd, J.G., 1965. Stratigraphical nomenclature of Iranian Oil Consortium agreement area: American Association of Petroleum Geologists Bulletin, 49: 2182-2245.

Jones, B., Manning, A.C., 1994. Comparison of geochemical indices used for the interpretation of paleoredox conditions in ancient mudstones. Chemical Geology, 111: 111-129.

Lewan, M.D., 1984. Factors controlling the proportionality of vanadium to nickel in crude oils. Geochimica et Cosmochimica Acta, 48: 2231-2238.

Lewan, M.D., Maynard, J.B., 1982. Factors controlling enrichment of vanadium and nickel in the bitumen of organic sedimentary rocks. Geochimica et Cosmochimica Acta, 46: 2547-2560.

Li. D., Li, R., Xue, T., Wang, B., Liu, F., Zhao, B., Zhao, D., 2018. Characteristic and geological implications of major elements and rare earth elements of Triassic Chang 7 oil shale in Tongchuan City, Southern Ordos Basin (China). Minerals, 8(4): 157.

Long, J., Luo, K., 2017. Trace element distribution and enrichment patterns of Ediacaran-early Cambrian, Ziyang selenosis area, Central China: constraints for the origin of selenium. Journal of Geochemical Exploration, 172: 211-230.

Malaza, N., Liu, K., Zhao, B., 2013. Facies analysis and depositional environments of the late Palaeozoic coal-bearing Madzaringwe Formation in the Tshipise-Pafuri Basin, South Africa. International Scholarly Research Notices,1-11.

McCord, D.R., 1974. Ahwaz Field Asmari Reservoir: Oil Service Company of Iran, Internal Report.

McLennan, S.M., Hemming, S.R., McDaniel, D.K., Hanson, G.N., 1993. Geochemical approaches to sedimentation, provenance, and tectonics. In: Johnsson, M.J., Basu, A. (Eds.), Processes Controlling the Composition of Clastic Sediments. Geological Society of American Special Paper 284: 21-40.

Mehrabi-Rashnou, A., 2017. Investigating concentration of rare elements including nickel and vanadium in Ahwaz oilfield. M.Sc. thesis, Shahid Chamran University of Ahwaz, Ahwaz, Iran, 139 pp. (in Persian with English abstract)

Mortazavi, M., Mossavi-Harami, R., Mahboubi, A., Nadjafi, M., 2013. Geochemistry of the Late Jurassic-Early Cretaceous shales (Shurijeh Formation) in the intracontinental Kopet-Dagh Basin,

northeastern Iran: implication for provenance, source weathering, and paleoenvironments. Arabian Journal of Geosciences, 7 (12): 5353-5366.
Motiei, H., 1993. Stratigraphy of Zagros. Geological Survey of Iran, Tehran, 583 pp.
Navidtalab, A., Sarfi, M., Enayati-Bidgoli, A., Yazdi-Moghadam, M., 2020. Syn-depositional continental rifting of the Southeastern Neo-Tethys margin during the Albian-Cenomanian: evidence from stratigraphic correlation. International Geology Review, 62: 1698-1723.
Navidtalab, A., Rahimpour-Bonab, H., Huck, S., Heimhofer, U., 2016. Elemental geochemistry and strontium-isotope stratigraphy of Cenomanian to Santonian neritic carbonates in the Zagros Basin, Iran. Sedimentary Geology, 346: 35-48.
Piryaei, A., Reijmer, J.J.G., Borgomano, J., van Buchem, F.S.P., 2011. Late cretaceous tectonic and sedimentary evolution of the bandar abbas area, fars region, southern Iran. Journal of Petroleum Geology, 34: 157-180.
Piryaei, A.R., Reijmer, J.J.G., Vanbuchem, F.S.P., Yazdi-Moghadam, Sadouni, J., Danelian, T., 2010. The influence of Late Cretaceous tectonic processes on sedimentation patterns along the northeastern Arabian plate margin (Fars Province, SW Iran). Geological Society of London, Special Publication, 330 (1): 211-251.
Potter, P.E., 1978. Petrology and chemistry of modern big river sands. Journal of Geology 86: 423-449.
Rabbani, A.R., Bagheri-Tirtashi, R., 2010. Hydrocarbon source rock evaluation of the Super Giant Ahwaz oilfield, SW Iran. Australian Journal of Basic Applied Sciences, 4 (5): 673-686.
Rimmer, S.M., 2004. Geochemical paleoredox indicators in Devonian-Mississippian black shales, Central Appalachian Basin (USA). Chemical Geology, 206 (3): 373-391.
Roozpeykar, A., Maghfouri-Moghaddam, I., 2016. Benthic foraminifera as biostratigraphical and paleoecological indicators: an example from Oligo-Miocene deposits in the SW of Zagros basin, Iran. Geoscience Frontiers, 7 (1): 125-140.
Roser, B.P., Korsch, R.J., 1988. Provenance signatures of sandstone-mudstone suites determined using discriminant function analysis of major-element data. Chemical Geology, 67: 119-139.
Roser, B.P., Korsch, R.J., 1986. Determination of tectonic setting of sandstone-mudstone suites using SiO_2 content and K_2O/Na_2O ratio. Journal of Geology, 94: 635-650.
Sadeghi, R., Vaziri-Moghaddam, H., Taheri, A., 2009. Biostratigraphy and paleoecology of the Oligo-Miocene succession in Fars and Khuzestan areas (Zagros Basin, SW Iran). Historical Biology, 21 (1-2): 17-31.
Safi, M., 2019. Trace and rare earth elements geochemistry and genesis of petroleum source rocks from the Ahwaz oilfield. Unpublished MSc Thesis, Shahrood University of Technology, Shahrood, 97 pp. (in Persian with English abstract)
Sharland, P.R., Archer, R., Casey, D.M., Davies, R.B., Hall, S.H., Heward, A.P., Horbury, A.D., Simmons, M.D., 2001. Arabian Plate sequence stratigraphy. GeoArabia, Special Publication, 2: 1-371.
Sherkati, S., Letouzey, J., 2004. Variation of structural style and basin evolution in the central Zagros (Izeh zone and Dezful Embayment), Iran. Marine and Petroleum Geology, 21: 535 - 554.
Stöcklin, J., 1968. Structural history and tectonics of Iran: a review of American Association Petroleum Geology Bulletin 52: 1229-58.
Takin, M., 1972. Iranian geology and continental drift in the Middle East. Nature, 235: 147-50.
Taylor, S.R., McLennan, S.M., 1985. The continental crust: its composition and evolution. Blackwell Scientific Publications, Oxford, 312 pp.
Thompson, M., Howarth, R.J., 1978. A new approach to the estimation of analytical precision. Journal of Geochemical Exploration, 9: 23-30.
Tissot, B.P., Welte, D.H., 1984. Petroleum formation and occurrence. Second Ed., Springer-verlag, Berlin, Heidelberg, New York, Tokyo, 699 pp.
Udo, O.T., Ekwere, S., Abrakasa, S., 1992. Some trace metal in selected Niger Delta crude oils: application in oil-oil correlation studies. Journal of Geology and Mining Research, 28: 289-291.
Valinejad-Khiaban, N., 2015. Geochemical investigating of vanadium and nickel concentrations in Mansuri and Ab-Teymour oilfields, Dezful Embayment, Khuzestan Province. M.Sc. thesis, Tabriz University, Tabriz, Iran. (in Persian with English abstract).
Wang, S.F., Dong, D.Z., Wang, Y.M., Li, X.J., Huang, J.L., Guan, Q.Z., 2015. Sedimentary geochemical proxies for paleoenvironment interpretation of organic-rich shale: a case study of the lower Silurian

Longmaxi Formation, southern Sichuan basin, China. Journal of Natural Gas Science and Engineering, 28: 691-699.

Wignall, P.B., Twitchett, R.J., 1996. Oceanic anoxic and the end Permian mass extinction. Science, 272: 1155-1158.

Xie, G.L., Shen, Y.L., Liu. S.G., Hao, W.D., 2018. Trace and rare earth element (REE) characteristics of mudstones from Eocene Pinghu Formation and Oligocene Huagang Formation in Xihu Sag, East China Sea Basin: implications for provenance, depositional conditions and paleoclimate. Marine and Petroleum Geology, 92: 20-36.

Zeinalzadeh, A., Moussavi-Harami, R., Mahboubi, A., Sajjadian, V.A., 2018. Source rock potential of the Early Cretaceous intervals in the Darquain field, Abadan Plain, Zagros Basin, SW Iran. Geosciences Journal, 22 (4): 569-580.